

PAPER • OPEN ACCESS

Study accuracy of a transportation system positioning of a test rig for automated mounting of luster terminals

Recent citations

- [Stiliyan Nikolov et al](#)

To cite this article: R K Dimitrova *et al* 2019 *IOP Conf. Ser.: Mater. Sci. Eng.* **659** 012031

View the [article online](#) for updates and enhancements.

Study accuracy of a transportation system positioning of a test rig for automated mounting of luster terminals

R K Dimitrova¹, V Zhmud², N N Petrov³ and T A Vakarelska⁴

¹ Technical University, Faculty of Mechanical Engineering, Blvd Kl. Ohridski 8, 1000 Sofia, Bulgaria

² NGTU, Novosibirsk, Russia

³ Technical University, Faculty of Mechanical Engineering, 8 Kl. Ohridski Blvd, 1000 Sofia, Bulgaria

⁴ Technical University, KEE, 8 Kl. Ohridski Blvd, 1000 Sofia, Bulgaria

E-mail: rkd@tu-sofia.bg

Abstract. A test rig for study of parameters of a process of automated assembly of luster terminals is designed and developed. The aim of the developed test rig is to study the accuracy of positioning of the transport system during the automated assembly process of luster terminals. On the basis of data collected during the experiments, reliability analysis of the whole system has been made.

1. Introduction

Subject to automation is a plastic luster terminal with twelve inputs/outputs and mounting holes. It consists of a body in which brass details are placed with threads, each having two screws. An automated assembly system test rig had been designed and manufactured. The design is based on the test and assembly rigs presented in [1, 2, 3, 4, 5, 6, 8]. It has the following main modules (Figure 1 and Figure 2):

- Magazine - collectors (MC) for each of the three different elements, which are assembled into a final product "luster terminal" - a total of 10 pieces;
- A linear conveyor (LC), which moves the elements between the different positions;
- Interceptors for Element B and Element B (element A is cut off by MC by LC);
- Module for carrying out technological operation (TO) - assembling by threaded connection of 6 pcs. Elements B to 3 pcs. Elements B in position 4.

After the production and purchase of all the necessary items, a test rig for the automated assembly of luster terminals is assembled. For programming of the stand the used program is "WinPISA 4.51" by "Festo" [7]. The input and output parameters are responsible for the information sent and received by all pickups, sensors and pneumatic cylinders, connected in the test rig. By using this information and depending on the value of each parameter, the blocks in the prepared block diagram are executed one after the other (Figure 5). Each individual block requires a specific value of one or several parameters in order to send the program signal for a subsequent operation to the test rig and to move to a next block where again the program will require specific values from the input parameters. After executing one program cycle, it starts again. Each pneumatic cylinder sends a signal of the position in



which it is located and this signal is constantly checked by the program. The same applies to the sensors responsible for the presence of elements in the MC. The test rig enters pause mode in case there are no items available in any of the MCs. The program set input and output parameters shown in Figure 3 and Figure 4.

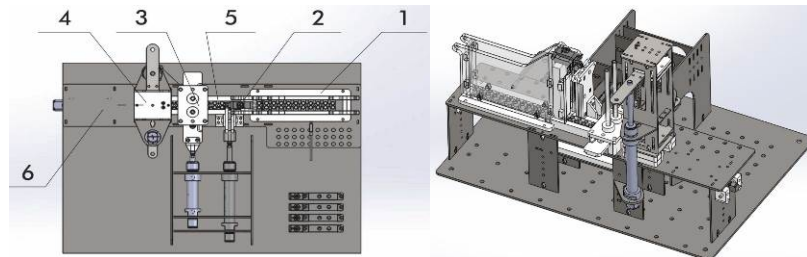


Figure 1. 3D model of a test rig of automated luster terminal mounting [3]: 1 - MC; 2 - MC with interceptor; 3 - Two MCs with interceptor; 4 - Operating position for mounting screw-type element; 5 - Linear conveyor.

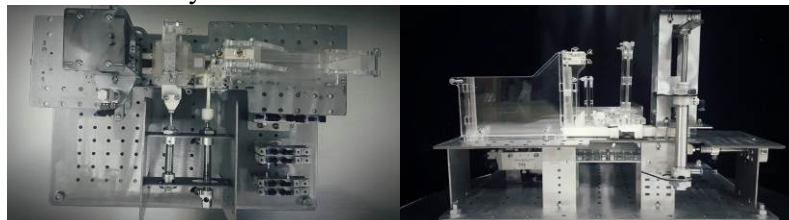


Figure 2. General view of the test-rig [3].

Variable	Mapping	Channel	Address	Type	Default Value	Unit	Description
		Onboard Input	%I80				CECC's onboard digital inputs
		Byte0	%I80	BYTE			
*nalchie_ms1		Bit0	%IX0.0	BOOL			fast input
*nalchie_ms2		Bit1	%IX0.1	BOOL			fast input
*nalchie_ms3		Bit2	%IX0.2	BOOL			
*count1		Bit3	%IX0.3	BOOL			
*s_ms1_b		Bit4	%IX0.4	BOOL			
*s_ms1_f		Bit5	%IX0.5	BOOL			
*s_ms2_b		Bit6	%IX0.6	BOOL			
*s_ms2_f		Bit7	%IX0.7	BOOL			
		Byte1	%I81	BYTE			
*s_ms3_b		Bit0	%IX1.0	BOOL			
*s_ms3_f		Bit1	%IX1.1	BOOL			
*s1_otv		Bit2	%IX1.2	BOOL			
*s2_otv		Bit3	%IX1.3	BOOL			
*start		Bit4	%IX1.4	BOOL			
*stop		Bit5	%IX1.5	BOOL			

Figure 3. Input parameters [3].

Variable	Mapping	Channel	Address	Type	Default Value	Unit	Description
		Onboard Output	%Q80				CECC's onboard digital outputs
		Byte0	%Q80	BYTE			
*c_ms1		Bit0	%QX0.0	BOOL	FALSE		
*c_ms2		Bit1	%QX0.1	BOOL	FALSE		
*c_ms3		Bit2	%QX0.2	BOOL	FALSE		
*c1_otv		Bit3	%QX0.3	BOOL	FALSE		
*c2_otv		Bit4	%QX0.4	BOOL	FALSE		
*rboot		Bit5	%QX0.5	BOOL	FALSE		
		Bit6	%QX0.6	BOOL	FALSE		
		Bit7	%QX0.7	BOOL	FALSE		

Figure 4. Output parameters [3].

A block diagram of the operations performed in accordance with the operating cycle of the test rig is shown in Figure 5.

2. Methodology for experimental studies

When performing a certain number of observations or measurements on the subject, the results are obtained x_1, x_2, \dots, x_q , which form an elementary statistical aggregate (elementary statistical order) of volume n . Observed or measured values are the final number of independent random variables that have the same distribution law as the random variable X . The values x_1 , are called variations, and their ranking in ascending order - ranging order [1, 2, 3].

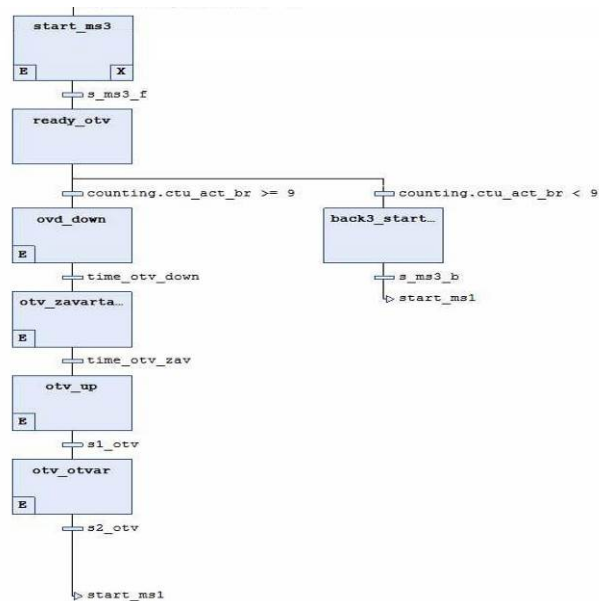


Figure 5. Block diagram of the program used [3].

The resulting statistical set of values x_i , ($i = 1, 2, \dots, q$) of the random value X together with the absolutes v_i and relative frequencies f_i form a statistical distribution law. The conversion count of X determines the absolute frequencies - v_i , and their relationship to volume determines the relative frequencies f_i . In that:

$$\sum_{i=1}^q v_i = n, \sum_{i=1}^q \frac{v_i}{n} = 1 \quad (1)$$

For a continuous random quantity, the statistic is broken down into classes (groups, orders) that are usually of equal lengths of intervals. In this way, an interval statistical sequence is obtained with k - class. The length of the interval $h = x_i - x_{i-1}$ ($i = 1, 2, \dots, k$) is determined by the dependence:

$$h = \frac{x_{max} - x_{min}}{k} = \frac{\hat{R}}{k} \quad (2)$$

Processing of experimental data x_i ($i = 1, 2, \dots, n$) from small samples is performed in the following sequence of calculation, analysis, comparison of the relevant parameters (parameters):

- Variation order is created.
- The values of the numerical characteristics are determined.
- Absolute and relative mean errors for individual numerical characteristics are determined.
- The maximum absolute and relative errors of the individual numerical characteristics are determined by replacing the theoretical with the empirical values.
- Trusted limits and confidence intervals are determined at a preset confidence probability y .
- The minimum sample size required is determined.

Statistical analysis and processing of experimental data x_i ($i = 1, 2, \dots, n$) from large samples is performed in the following order:

- An interval statistic line is compiled and the range R is determined, the length of the interval h and the number of classes k .
- The statistical set is represented graphically by an empirical distribution function, histogram and polygon.
- The values of the numerical characteristics are determined.
- The absolute and relative weighted errors for the individual numerical characteristics of disposition and scattering are determined.
- The values of the numerical characteristics of the moments (conditional start and center moments) are determined.
- Statistical estimates of asymmetry and excess (skewness and kurtosis) are determined.

By the type of the histogram and the polygon of the statistical law, the empirical values of asymmetry and excess and the physical essence and the physical sequence for obtaining and measuring the random quantity can be made the choice of the theoretical distribution law. For a more accurate assessment of the similarity of the experimental and theoretical distribution, the theoretical frequencies are calculated and a theoretical curve is constructed on the same scale [1, 2, 3].

2.1. Processing of results from engineering studies under "normal distribution"

The methodical sequence for constructing a normal distribution, which is most often subordinated to the distribution of random variables in all statistics, is subdivided into k classes with equal lengths of intervals h ; apply the exact values of the lower and upper limits of the classes $x_{i-1} \div x_i$; the average of each class and the corresponding frequencies are determined v_i [1, 2, 3]:

- the arithmetic mean is calculated:

$$\bar{x} = \frac{\sum_{i=1}^k \bar{x}_i v_i}{\sum_{i=1}^k v_i} \quad (3)$$

- the corrected dispersion and the mean quadratic deviation are calculated:

$$s^2 = \frac{\sum_{i=1}^k \bar{x}_i^2 v_i}{\sum_{i=1}^k v_i} - \bar{x}^2 \quad (4)$$

- Differences are determined for each class $|\bar{x}_i - \bar{x}|$ and the values of the normalized deviations:

$$t_i = \frac{|\bar{x}_i - \bar{x}|}{s} \quad (5)$$

- The tabulated values of $f(t_i)$ for the found values of it are determined;
- the theoretical frequencies are determined and round up to an integer:

$$v_i = \frac{nh}{s} f(t) \quad (6)$$

The experimental (polygon) and the theoretical (equalized) distribution by normal law are constructed on the same scale: the differences between the experimental and the theoretical distribution curve are determined and the error is evaluated [1, 2, 3].

2.2. Result processing under the "exponential distribution" hypothesis

The methodology includes the following steps:

Step 1: Chronometry of fault-free time and time of failure.

Step 2: A statistical hypothesis on the exponential law of distribution of the probability of faultless work is adopted.

Step 3: Based on experimental data, the number of intervals for non-faultless operation n is determined and the limits for their modification t_i , $i = n$.

The time of faultless operation m_{mid} is calculated according to:

$$m_{mid} = \frac{\sum_{i=1}^n (\Delta N_i t_i)}{n} \quad (7)$$

- Calculation of the statistical probability curve for faultless operation $P_i(t_i)$

$$P_i(t_i) = \frac{n - \sum_{i=1}^n (\Delta N_i t_i)}{n} \quad (8)$$

- Calculation of the reliability function $P(t)$

$$P(t) = e^{-\frac{t}{m_{mid}}} \quad (9)$$

- Determining the average withdrawal time T_v

$$T_v = \frac{\sum_{i=1}^n (\Delta N_i t_{mid})}{\sum_{i=1}^n (\Delta N_i)} \quad (10)$$

where: t_{mid} is the average of the time interval

- We define the failover flow parameter w

$$w = \frac{t_c}{m_{mid}} \quad (11)$$

where: t_c is cycling time

- Determination of actual productivity Q_f

$$Q_f = \frac{1}{t_c + t_{mid}} = \frac{m_{mid}}{t_c(m_{mid} + T_v)} \quad (12)$$

where: t_{mid} are the stays of AT in the execution of one cycle.

- The results of the experimental studies are presented in a table.
- The experimental curve for faultless operation $P_i(t_i)$ and the theoretical curve $P(t)$ are built.
- The error is determined and compared to the allowable one.

3. Conducting the experiments and processing the results of the experimental research

The following experimental studies are performed:

- Position accuracy of the transport system.
- Reliability of the automated mounting test rig.

3.1. Position accuracy of the transport system

Experimental studies have been conducted to determine the positioning accuracy at different transfer speeds of the linear conveyor. Figure 6 shows the schematic diagram of the test setup for measuring positioning accuracy. The results of the experiments are shown in Table 1.

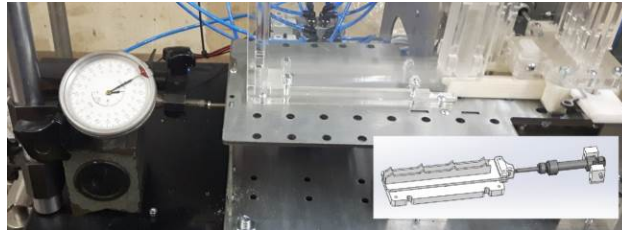


Figure 6. Positioning accuracy measurement.

$$\Delta X_{\text{mid}} = \bar{x} = 2,5 \qquad \sigma = \sqrt{\frac{21,25}{10}} = 1,458$$

The normal distribution function Y is calculated using the formula:

$$Y = \frac{1}{\sqrt{2\pi}\sigma} e^{-\frac{(\Delta x_{\text{mid}} - \Delta x_{\text{imid}})^2}{2\sigma^2}} \quad (13)$$

Table 1. Experimental research results.

Nº of the interval	Interval [microns]	Frequency of occurrence n	$(\Delta x_{\text{mid}} - \Delta x_{\text{imid}})$	$(\Delta x_{\text{mid}} - \Delta x_{\text{imid}})^2$	Y
1	-2 ÷ -1,5	3	2.5	6.25	0.00036
2	-1,49 ÷ -1	5	2	4	0.00389
3	-0,09 ÷ -0,5	10	1.5	2.25	0.02503
4	-0,49 ÷ 0	14	1	1	0.09454
5	0,01 ÷ 0,5	28	0.5	0.25	0.20985
6	0,51 ÷ 1	16	0	0	0.27374
7	1,01 ÷ 1,5	12	-0.5	0.25	0.20985
8	1,51 ÷ 2	8	-1	1	0.09454
9	2,01 ÷ 2,5	3	-1.5	2.25	0.02503
10	2,51 ÷ 3	1	-2	4	0.00389

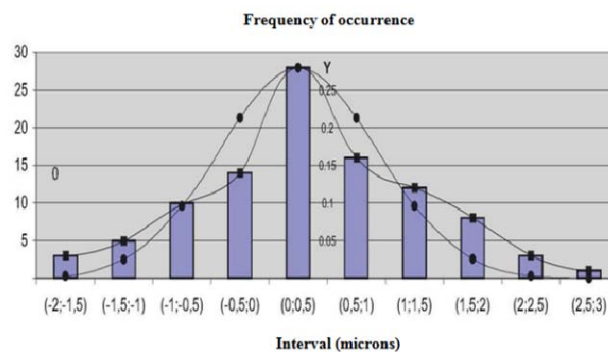


Figure 7. Experimental results for positioning accuracy.

Figure 7 shows the processed experimental results for positioning accuracy of the transport system of the test rig in graphical form. The graph shows that the accuracy of the positioning is about +2,5 [microns], which corresponds to the positioning accuracy for mounting operations.

3.2. Determination of the reliability of the test rig for the automated assembly of luster terminals.

Experimental tests have been carried out for the reliability of the automated assembly system and the results are shown in Table 2.

Table 2. Experimental results for the reliability of the test rig.

№ of the interval	Interval boundaries [min]	Average interval value(t_i)	ΔN_i	$\sum \Delta N_i, i=1 \div n$	$N - \sum \Delta N_i, i=1 \div n$	$P_i(t_i)$	t/m_{mid}	$P(t)$
1	0 - 2	1	3	3	23	0,88	0,10	0,92
2	2 - 4	3	2	5	21	0,81	0,30	0,72
3	4 - 6	5	4	9	17	0,65	0,51	0,58
4	6 - 8	7	1	10	16	0,62	0,71	0,47
5	8 - 10	9	2	12	14	0,54	0,91	0,36
6	10 - 12	11	3	15	11	0,42	1,12	0,25
7	12 - 14	13	5	20	6	0,23	1,32	0,18
8	14 - 16	15	2	22	4	0,15	1,52	0,12
9	16 - 18	17	1	23	3	0,12	1,73	0,05
10	18 - 20	19	3	26	0	0,00	1,93	0,02

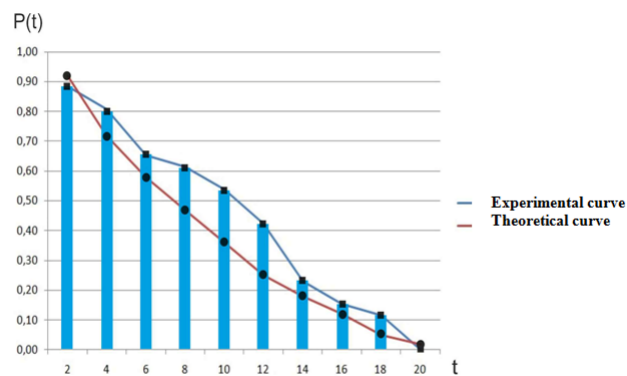


Figure 8. Results of experimental reliability studies.

On Figure 8 a graphical interpretation of the experiment results is presented. It can be seen that the error between the statistical and theoretical reliability curves is small, i.e. the two curves almost coincide.

For the automated assembly test rig under consideration:

$$m_{mid} = \frac{256}{26} = 9,84 \text{ [min]}$$

$$K_G = \frac{T_w}{T_w + T_v} = 0,97$$

where $T_w = m_{mid}$; T_v – average recovery time after failure;

The coefficient $K_G = 0,97$ (for $K_{Gmin} = 0,8$), which fully satisfies the operational reliability requirements.

4. Conclusion

- A test rig for automated luster terminals mounting is developed.

- From the experimental tests for the positioning accuracy of the transport system can be seen that the positioning accuracy is around +2,5 [microns], which corresponds to the positioning accuracy for mounting operations.
- From the experimental tests carried out for the reliability of the developed test rig for automated mounting of luster terminals is seen that the coefficient $KG = 0,97$ (for $KG_{min} = 0,8$), which fully satisfies the operational reliability requirements.
- The results of experimental studies that can be used in engineering practice are processed.

References

- [1] Dimitrov B S, Dimitrov L, Dimitrova R and Nikolov S 2019 Examination of the process of automated closure of containers with screw caps, *Studies in Systems, decisions and control*, **199** 502-514
- [2] Petrov N N 2016, *Tipovi efektivni resheniya za avtomatizatsiya na montazha na vyzli ot elektronnoto proizvodstvo (Efficient automation solutions for the assembly of electronic manufacturing units)*, Technical University of Sofia, Doctoral Thesis
- [3] Jiang Z, Harrison D K and Cheng K 2002 An integrated concurrent Engineering approach to the design and manufacture of complex components, *International Journal of Advanced Manufacturing Technology* **20**(5) 319 – 325
- [4] Sarkis J and Parsaei H 2011, *Advanced Manufacturing Systems - Strategic Management and Implementation*, Springer
- [5] Wang Q, Sowden M and Mileham A R 2013 Modelling human performance within an automotive engine assembly line, *International Journal of Advanced Manufacturing Technology* **68**(1) 141-148
- [6] Festo Didactic, *WinPisa for SPC 200*, <https://www.festo-didactic.com/us-en/products/software-e-learning/programming-software/winpisa-for-spc-200.htm?fbid=dXMuZW4uNTc5LjE3LjE4LjU2Ni4zNzUy> (accessed on Jan. 2018)
- [7] Dimitrov V L, Michalopoulos D, Apostopoulos C and Neshkov T 2009 Investigation of contact fatigue of high strength steel gears subjected to surface treatment. *Journal of Materials Engineering and Performance* **18** (7) 939-946
- [8] Tomov K P 2017 Increasing the efficiency of automation of production processes by reporting the parameters of the parts' flow, *TEM Journal* **6** (3) 484-487
- [9] Guergov S 2005 *Mathematical Modelling of a Flexible Multifunctional Manufacturing System for Mechanical Treatment*, 2nd International Conference on Manufacturing Engineering (ICMEN), Kassandra-Khalkidhiki, Greece, October 5-7, 781-790